

Contents lists available at ScienceDirect

Pattern Recognition

journal homepage: www.elsevier.com/locate/pr



Color perception of diffusion tensor images using hierarchical manifold learning



Xianhua Zeng*, Shanshan He, Weisheng Li

Chongqing Key Laboratory of Computational Intelligence, College of Computer Science and Technology, Chongqing University of Posts and Telecommunications, Chongqing 400065, China

ARTICLE INFO

Keywords: Diffusion tensor images High dimensional data Nonlinear dimensionality reduction Color perception Algebraic multigrid Multi-scale graph partitioning

ABSTRACT

The color perception of Diffusion Tensor Images (DTI) by using voxel-based statistical analysis suffers from high computational cost and vague regional structure. To address these issues, we therefore propose a novel approach for color perception of DTI based on hierarchical manifold learning. First, the selection of the representative nodes as seeds within similar region to build them into the bottom-to-up hierarchical structure is derived from the algebraic multigrid and multi-scale graph partitioning. Next, the low-dimensional coordinates of the top-layer seeds are calculated using manifold-based techniques with a new distance metric and mapping of these coordinates into the RGB color space. Last, the color perception of DTI is obtained through interpolating the seeds to the bottom layer of all nodes. The experimental results demonstrate that the proposed algorithm can reduce the computation complexity from $O(N^3)$ (based on algorithms in the literature (Ghassan et al., 2011 [9])) to $O(N^2)$ and highlight the different regional structures of the brain via color perception of variation.

1. Introduction

The novel technology of Diffusion Tensor Imaging (DTI) has been developed since the end of the twentieth century from its use in Magnetic Resonance Imaging. This technology provides significant information for the brain tissue micro-structure based on diffusion of water molecules in vivo [1,2]. Note that DTI, currently one of the primary tools in brain imaging, is a noninvasive tool that is used to study the white matter structure of the brain to diagnose preterm infant brains [3] and the development of central nervous system [4]. Unlike ordinary medical images, each pixel of a DTI image corresponds to a Diffusion Tensor (DT). DT is a symmetric 3×3 matrix, or second-order rank 3 diffusion tensors with 6 unique elements, which represents the water molecules diffusion at the current point. Furthermore, DTs must be Positive Semi-Definite (PSD).

High-dimensional and complex structures exist in the brain that cause difficulties in visualization and subsequent processing of DTI images [5,6]. To detect the available pattern information and analyze the intrinsic structures, Machine Learning (ML) methods based on DTI dimensionality reduction have gradually become the research focus. In [7], Brun proposed a method for coloring DTI fiber traces using Laplacian Eigen-maps (LE) to enhance the perception fiber bundles and connectivity in the human brain. The results were similar fiber

bundles mapped to similar points in the low-dimensional RGB color space. However, the results only mapped the specific fiber trace into the RGB color space, rather than the medical images. Thus, this method has limited application prospects. In [8], Verma explored nonlinear dimensionality reduction methods ISOmetric feature MAPping (ISOMAP) to discover the valid structure and geometric characterization of DTI images. This method has been applied to research on the growth and development of the brain in mice. In [9], Hamarneh surveyed the ISOMAP algorithm to visualize the high-dimensional, manifold-valued DTI images that are faithful to the underlying DTI data. The approach highlighted the importance of distance preservation to render similar pixels with perceptual similar color, and vice versa. The above-mentioned methods regarding ISOMAP require the calculation of the shortest path between pixels, resulting in the main memory being the limiting issue [10]. In [11], a method was proposed that utilized the Locality Preserving Projections (LPP) algorithm for extracting the manifold structure effectively and capturing the statistical relationships among tensor image data. To improve the noise immunity of the method, in [12], Aarabi proposed a method relying on the Diffusion Map (DM) to meaningfully visualize the brain white matter by means of high dimensional diffusion tensor data mapped to a threedimensional space. However, these methods do not consider the overall regional structures of DTI; rather, they emphasize the color difference

E-mail addresses: zengxh@cqupt.edu.cn (X. Zeng), 925407206@qq.com (S. He), liws@cqupt.edu.cn (W. Li).

^{*} Corresponding author.

X. Zeng et al. Pattern Recognition 63 (2017) 583-592

between the pixels in DTI. In addition, in the literature [13], the DTI with measurement noise can exhibit noise-induced correlations among diffusion tensor measures. In the literature [14], a method was reported to overcome the shortcomings of some dimension reduction methods, which have the mistake neighbor points to the correct locations. The authors proposed a novel technique known as Trustworthy Stochastic Proximity Embedding (TSPE) based on Stochastic Proximity Embedding (SPE), which preserves the neighborhood relation to the true neighbors. However, the performance of this algorithm is not stable enough.

The methods that rely on manifold learning to reduce the dimensions and color perception without loss of information for DTI are becoming increasingly popular [15]. However, these approaches face two main challenges. One challenge is that the approaches have high computation complexity. Because the DTI with 6-D and thousands of pixels use manifold learning methods, high hardware requirements and computational burden are inevitable. Another challenge is that, after dimensionality reduction, the results focus on the color difference of pixels, making the regional structures of the DTI indistinct. To address these two issues, here, we describe a novel and efficient approach for color perception of DTI. Our algorithm builds the pixels into a hierarchy structure, which is derived from the Algebraic MultiGrid (AMG) [16] and multiscale graph partitioning [17]. Next, only a mere fraction of the pixels are used for dimensionality reduction and color perception. Finally, the representative seeds are interpolated to all of the pixels. The main contributions of this paper are: (a) the proposal of a new method that decreases the complexity of calculation compared with methods in the literature [9] from $O(N^3)$ to $O(N^2)$; (b) the proposed method includes a new metric to approximately estimate the distance among the representative seeds of the top-layer to avoid double counting; (c) the results have better regional structures, which enhance the image texture feature information and improve the visual effect for clinicians; (d) the proposed method improves the algorithm in the literature [17] and extends the color perception of medical images application.

The rest of this paper is organized as follows. In Section 2, a related method is introduced in detail. Section 3 first, we present an analysis of the rationality of the hierarchical structure and then provide a summary of the proposed algorithm. In Section 4, we present a series of experimental results. Finally, we describe the conclusion and the future work in Section 5.

2. Color perception of DTI based on ISOMAP

In the field of medical image processing, a problem is that the medical image data are embedded in a high-dimensional space. To visualize the manifold-valued medical image data and improve both the visual perception and the accuracy of diagnosis, Hamarneh proposed an approach involving distance-preserving reduce dimension (DPDR) [9] and color perception for DTI; this approach renders the different perceptual colors to accurately reflect the different high-dimensional pixel values. First, for the diffusion tensor images, the dimensions of each pixel are larger than the dimensions of the color space. Employing multi-dimensional scaling distance-preserving enables the mapping of the high-dimension DTI within the dimensions that can be perceived by humans. The goal is that, after dimensionality reduction, similar pixels should be rendered in a color that is as close as possible to the perception. The metric of any two high dimensional pixels is determined by their geodesic distance on the manifold. Second, the lower dimensional coordinates are mapped to a three-channel color space to enhance the perception of pixels. Finally, in the case that the relative distance of the pixels is not changed, the color perception of the diffusion tensor images can be obtained via rotation, translation, and scaling to maximize the color gamut and volume. For more details regarding color perception for DTI based on DPDR, please refer to literature [9].

The advantages of using distance-preserving dimensionality reduction to color perception DTI are that the results have color diversification among the pixels along with rich details. However, because the DPDR method uses isometric feature mapping, which requires calculation of the geodesic distance between pixels, the complexity and hardware requirements are high. The high computational cost will hinder the promotion of this method in clinical application. Furthermore, ISOMAP is a global mapping method, and in literature [9], ISOMAP focuses on the color differences among pixels via operation of an enormous dissimilarity matrix, so the different regional structures and image texture in DTI will not be obvious. We establish a hierarchical structure to achieve the purpose of reducing the computational cost from $O(N^3)$ to $O(N^2)$ and the color information of representative seeds is transformed to all pixels by neighbor relationship of all pixels, in order to highlight the regional structures. This hierarchy color perception method can overcome the shortcoming of high computational cost and the vague regional structure.

3. Color perception of diffusion tensor images using hierarchical manifold learning (CPDTI-HML)

Considering the rationality of the distance-preserving dimensionality reduction for coloring perception DTI and the corresponding detects, i.e., high computational cost and a lack of regional structures, we propose a method involving color perception of diffusion tensor images using hierarchical manifold learning named as CPDTI-HML. For every layer, we select the most valuable pixels as seeds, and then the selected seeds are pictured as candidate nodes on the next layer. The rest of the pixels can be processed in the same manner. By selecting the representative seeds, all pixels are built into a hierarchical structure. From the bottom to top, the method forms a pyramid, in which the most influential seeds are at the top, and all of the pixels are at the bottom [17]. The top-layer representative seeds using the multidimensional scaling (MDS) [19] method directly are mapped to a lower dimension space and then converted to the RGB color space before returning to all the pixels with color information by interpolating representative seeds from the top layer to the bottom layer. This hierarchy color perception method can overcome the shortcomings of high computational complexity and vague regional structures. An overview of the color perception of DTI using hierarchical manifold learning is shown in Fig. 1..

3.1. Selecting representative seeds of regional structures

To reduce the computational complexity and obtain the representative nodes of regional structures, our method selects the representative and influential nodes as seeds from all of the pixels at the current layer, which represent the main regional structures of DTI. Next, the selected nodes are regarded as candidate nodes on next layer. The rest of the nodes can be treated in the same manner. From the bottom to top it forms a pyramid, in which the most valuable seeds are at the top, and all of the pixels are at the bottom [17,18,20]. This process is able to retain those nodes with greater impact, while ignoring smaller effect of those similar nodes.

Let X_i i=1 to N be the original pixel point sets of diffusion tensors. A six-dimensional vector $I_i=(I_1,\,I_2,\ldots,I_6)$ represents six independent elements corresponding to the i-th pixel point X_i . First, constructing the k-neighborhood graph $G^{[0]}(V^{[0]},\,W^{[0]})$, $V^{[0]}$ being its set of all nodes, each corresponding to a pixel, with $W^{[0]}$ being the similarity matrix. $W_{ij}^{[0]}$ represents the weights along the edges connecting pixels i and j, to be determined as follows:

$$W_{ij}^{[0]} = \begin{cases} \exp(-\alpha ||I_i - I_j||_2), & I_j \in N_k(I_i) \text{ or } I_i \in N_k(I_j) \\ 0, & \text{otherwise} \end{cases},$$
 (1)

where $N_k(I_i)$ and $N_k(I_i)$ represent the k-nearest neighbor set of I_i and I_i ,

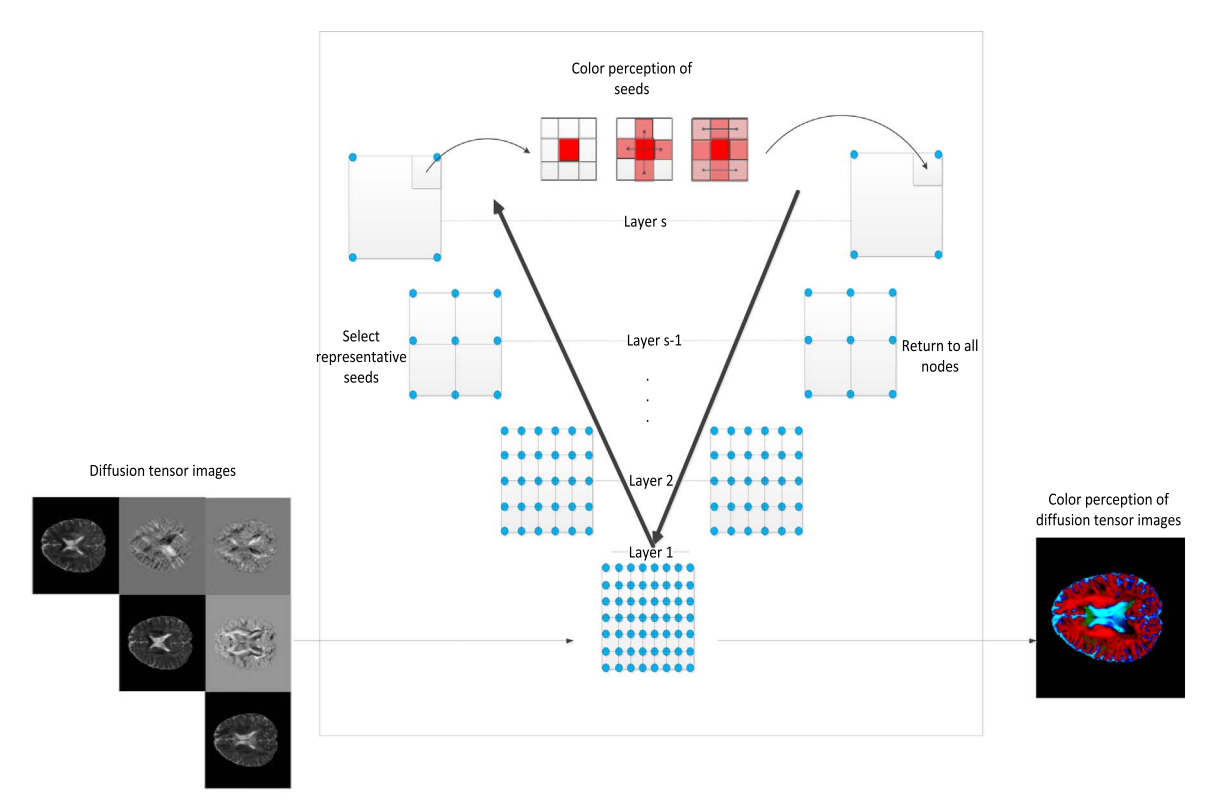


Fig. 1. Overview of the proposed method.

respectively, and α is the parameter of the kernel function.

The representative seeds must be selected to build a hierarchy structure, which represents the main structure information for different regions in DTI. The intuitive condition of selecting representative seeds is as follows. The representative seeds are strongly connected with the non-representative seeds in DTI. For the strong connection between two pixels, we utilize the simple similarity metric (under the inspiration of [17,18]). Without loss of generality, letting W denote the general mathematical notation of the similar matrix at any layer, before selecting the representative seeds, we define the strong connection between node i and node j with significant similarity as follows:

$$W_{ij} \ge \theta \ Max_{k \ne i} \{W_{ik}\}, \quad 0 < \theta \le 1, \tag{2}$$

where θ is the strength threshold, which reflects the strength of the relationship between neighbors. A node i strongly connected to node j in the DTI k-neighborhood graph means that the similarity between the two nodes is a great proportion of the maximum similarity between node i and its neighborhood nodes. In particular, in practical operation, node i is selected as the representative seed node if Eq. (2) is satisfied and the degree of the node i is larger than that of node j; otherwise, node j is selected.

Obviously, on the s-th layer of the bottom-to-top hierarchical structure, the selected representative seeds between the neighborhood layers should satisfy $V^{[s]} \subseteq V^{[s-1]}$, where s=1, 2, ..., N, and N denotes the layer number. Under the constraint of Eq. (2), each node in $V^{[s-1]}/V^{[s]}$ is strongly connected to $V^{[s]}$ [17]. In this manner, only the selected representative nodes with different regional structures are involved in the color perception in the next step, whereas the non-representative nodes are negligible. As a result, the amount of calculation is reduced and the region information of the DTI is emphasized.

After the representative nodes of the next layer are selected, the similarity metric between these representative nodes is kept to be as high as possible. Thus, for transforming the similarity among the different layers, we only need to establish a similarity transformation matrix inspired by the inter-layer interpolation matrix [17,20]. The essence of the transformation matrix is the following: if the similarity

among representative seeds exists in the lower layer, then we only need to retain the similarity, or else the similarity is calculated by the average similarity on all reachable paths. As a result, a reasonable definition of the similarity transformation matrix $P^{(s-1)}$ from the (s-1)-th layer to the s-th layer is described as follows:

$$\begin{cases} P_{ik}^{[s-1]} = \frac{W_{ik}^{[s-1]}}{\sum_{k} W_{ik}^{[s-1]}}, i \notin V^{[s]}, k \in V^{[s]} \\ P_{ii}^{[s-1]} = 1 \\ P_{ij}^{[s-1]} = 0, i \in V^{[s]}, j \neq i \end{cases}$$
(3)

As the above-defined transformation matrix $P^{[s-1]}$ between the two neighboring layers, the similarity matrix of representative nodes $W^{[s]}$ at the next layer can be described by the following formula:

$$W^{[s]} = P^{[s-1]T}W^{[s-1]}P^{[s-1]}$$
(4)

This strategy guarantees the transformation of the similarity matrix after constructing a hierarchical structure in an obvious manner:

$$W^{[s]} = P^{[s-1]T} P^{[s-2]T} \dots P^{[1]T} P^{[0]T} W^{[0]} P^{[0]} P^{[1]} \dots P^{[s-2]} P^{[s-1]}$$
(5)

After we obtain the representative nodes and their corresponding similarity matrix on the top layer, the intrinsic 3-dimensional coordinates corresponding to the RGB color space are obtained by dimensionality reduction while preserving the distance metric, as described in Section 3.2.1. In addition, we can return bottom-layer to obtain the 3-dimensional representations of all pixels using the transformation matrix sequence $P^{\{0\}}P^{\{1\}}...P^{\{s-2\}}P^{\{s-1\}}$, approximated as the inter-layer interpolation matrix in Section 3.3.

3.2. Color perception of seeds

When building the hierarchical structure for all of the pixels, we only need to reduce dimensionality for the representative seeds on the top layer directly using the manifold learning method such that the distance among the seeds is maximally reserved to obtain the intrinsic three dimensional coordinates. For some representative seeds, we

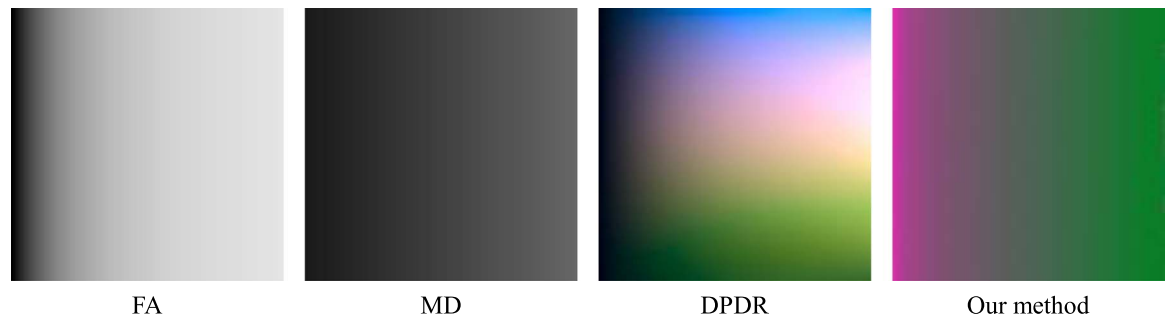


Fig. 2. Display of the simulated DTI data results obtained by FA, MD, DPDR and our method. FA captures the variability along the horizontal direction, and MD does not capture any changes. DPDR can present the changes from the horizontal direction and the vertical direction. Our method captures changes in the horizontal direction.

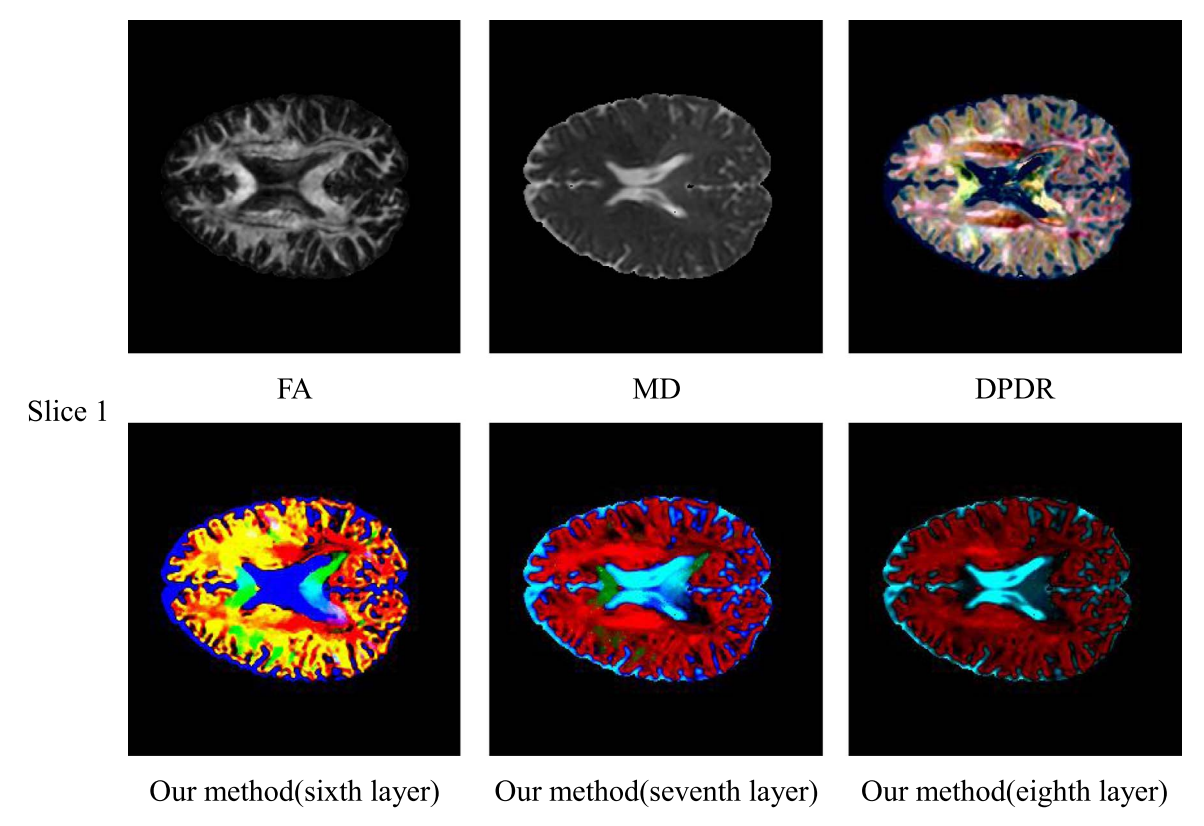


Fig. 3. Display of the real DTI data results obtained by FA, MD, DPDR and our method. FA and MD are scale images, i.e., the pixels do not have color information. DPDR and our approach have color information, but our approach reduces the amount of computation and emphasizes the regional structures.

provide some color information in the RGB color space and seek a rotation scale in which the color information should be as close as possible to the lower coordinates of the corresponding seeds. The other seeds are transformed by rotation scale to maximize the color gamut and volume among the representative seeds, and then the perceptual color differences are highlighted and the color information between the representative seeds is enriched. The principle guarantees that similar seeds will be represented by similar colors, whereas different seeds will be represented by dissimilar colors. In summary, the difference between the seeds can be expressed by different colors.

3.2.1. Distance measure for the seeds

The use of distance-preserving manifold learning for the representative seeds to reduce the dimensionality requires the distance between seeds on the top layer. From the bottom layer to the top layer, a large number of pixels are neglected. Because representative seeds include parts of all of the pixels, computing the Euclidean distance or geodesic distance directly for the top-layer seeds is inappropriate because of the great error between the real distance and the directly computed

distance along with double counting. A simple strategy is the use of the similarity matrix of all of the nodes to compute the distance by the exponential function for the inverse operator of the similarity computation. Through the inter-layer transformation matrix P, the similarity matrix of the representative seeds is transferred on the upper layer. The other seeds are processed until the top layer is reached in the same manner. After we obtain the top-layer representative seeds and their similarity matrix, we only need to take the logarithm function of the similarity matrix of the top-layer of the representative seeds to obtain the solution, thus approximately estimating the distance of the seeds. Using the proposed tactic, we can avoid repeated calculation and accurately estimate the distance of seeds. Thus, the distance for representative seeds is defined as follow:

$$D\left(I_{i}I_{j}\right) \approx -\frac{1}{\alpha}\log(W_{ij}^{[n]}),\tag{6}$$

where $W^{[n]}$ denotes the similarity matrix of the seeds in the goal layer n, and D denotes distance matrix corresponding to the representative seeds. α is the parameter of the kernel function corresponding to Eq. (1).

X. Zeng et al. Pattern Recognition 63 (2017) 583-592

3.2.2. Color transformation at the representative seeds

For the representative seeds, the MDS [19] is used for distancepreserving mapping to obtain the three-dimension coordinates. Next, the RGB color space is adopted as the range of the MDS mapping. To accomplish the color perception of the seeds, we must provide local color cues for some representative seeds and then expand the local color information to the whole seeds. The first step is to set up different color information for some of the representative seeds. Next, from the color information and the three dimensional coordinate corresponding to the given seed, we can seek the rotation-scaling transformation that ensures the color information and the 3-dimensional coordinates are as close as possible. The remaining seeds are rotated to obtain the color information, thus expanding the color gamut and volume. The method both renders seeds with color and provides different color information for different seeds based on perception. From the known color information C_s and the corresponding 3-dimensional coordinates U_s , we seek the rotation-scaling matrix R. These processes are first to centralize the basic color information:

$$\mu_{C_s} = \frac{1}{p} \sum_{i=1}^{p} C_s \tag{7}$$

Where p denotes the number of representative seeds with color information, and C_s denotes the known color information of the given representative seeds.

$$\mu_{U_s} = \frac{1}{p} \sum_{i=1}^{p} U_s \tag{8}$$

Where U_s denotes three-dimensional coordinates of the given representative seeds. Note that the essence of rotation-scaling is that the color information C_s should be as close as possible to the three-dimensional coordinates U_s of the corresponding seeds, i.e., their covariance is maximized:

$$COV = \frac{1}{p} \sum_{i} (C_s - \mu_{C_s}) (U_s - \mu_{U_s})^T COV = UDV^T$$
(9)

If the singular value decomposition of the covariance matrix COV is UDV^T , then $UU^T = VV^T = I$, $D = diag(d_i)$, $d_1 \ge d_2 \ge d_3$ and d_i is the i-th largest Eigenvalue of the matrix COV. To minimize the error between the known color information C_s and the transformation RU_s from the 3-dimensional coordinates U_s , the rotation-scaling transformation R must be satisfied with the formula:

$$R = USV^{T} \tag{10}$$

where the S is determined by:

$$S = \begin{cases} I & , |Cov| \ge 0 \\ diag(1, 1, -1) & , otherwise \end{cases}$$
 (11)

where, for the determinant |Cov| > 0, the same-direction rotation is used; otherwise the different direction rotation is used.

Via the above computation, R represents the rotation-scaling transformation from the 3-dimensional coordinate space to the RGB color space. The three-dimensional coordinates of all of the seeds at the top layer can be rotated and scaled to obtain the corresponding RGB colors by the matrix R, and then the color information of the whole diffusion tensor images is obtained by the color clue of the top layer, as described in the following section.

3.3. Color perception of all nodes

After obtaining the color perception of the representative seeds on the top layer, the next step is interpolation to all of the pixels on the bottom layer from representative seeds on top layer. The purpose of the interpolation is to map the color information from the representative seeds to all of the nodes, thus rendering the pixels of the diffusion tensor images with color. Similar to the selection of the representative seeds, we also utilize the transformation matrix as

the same inter-layer interpolation matrix P for every layer to return all of the pixels. More significantly, a similar region should be perceived as being similar in color, and vice versa. The interpolation formula is defined as follows:

$$Y^{s-1} = P^{(s-1)}Y^{(s)} (12)$$

where $Y^{[s]}$ denotes the representative seeds with color information on the upper layer, and $Y^{[s-1]}$ denotes seeds with the color information on the next layer. The rest of the layers can be processed in the same manner until the bottom layer nodes are assigned color information, i.e.,

$$Y^{[0]} = P^{[0]}P^{[1]} \dots P^{[s-2]}P^{[s-1]}Y^{[s]}$$
(13)

In this manner, using the transformation matrix sequence $P^{[0]}P^{[1]}...P^{[s-2]}P^{[s-1]}$, all of the pixels of the DTI can be perceived based on the color information, with similar regions having similar colors.

3.4. Summary of the proposed algorithm

Summarizing the above analysis, for solving the high computational cost problem and enhancing the regional structures of the diffusion tensor images, we proposed the hierarchical color perception algorithm on DTI. By constructing the bottom-to-top hierarchical structure for all of the pixels, only the most representative seeds on the top layer retaining the geometric structure are mapped to the three-dimensional space using MDS. Next, the three-dimensional coordinates of seeds are converted to the RGB color space to render the similar seeds with color as similar as possible and different seeds with dissimilar colors. The color information of the top layer seeds is returned to all of the pixels via the inter-layer interpolation matrix, thus obtaining the color DTI with regional structure saliency from high-dimensional diffusion tensor data. The main procedures of the proposed method are summarized in Algorithm 1.

Algorithm 1. : (CPDTI-HML Algorithm) Color Perception of Diffusion Tensor Images Using Hierarchical Manifold Learning.

Input: Diffusion tensor images data

Output: Color diffusion tensor images

Step 1, DTI pre-processing. // Let 6-D matrix with size $m \times n$ of diffusion tensor images pull a column vector to form a matrix X: $(mn) \times 6$.

Step2, Construct *k*-neighborhood graph. // Construct *k*-neighborhood graph $G^{[0]} = (V^{[0]}, W^{[0]})$ of matrix $X, V^{[0]}$ being its set of all nodes, each corresponding to a pixel. The similarity matrix of all pixels is given by $W^{[0]}$ using Eq. (1).

Step3, Build a bottom-to-top hierarchical structure of all pixels using the following operation.

for s=1: n //construct $G^{[s]}$ from $G^{[s-1]}$ to select the representative seeds $V^{[s]}$:

(1) Select the set of representative seeds $V^{[s]}$ as the candidate nodes of the next layer from

 $V^{[s-1]}$, so that $V^{[s-1]}/V^{[s]}$ is strongly connected to $V^{[s]}$.

- (2) Calculate the inter-layer interpolation matrix $P^{[s-1]}$ using Eq. (3).
- (3) Update the similarity matrix $W^{[s]}$ of the selected seeds $V^{[s]}$ using Eq. (4).

if the number of representative seeds $V^{[s]}$ is less than the allowed minimum seeds

exit end if

end for

Step4, Obtain the distances between the top-layer seeds. // Estimate the distance between the representative seeds on the top layer n utilizing Eq. (6).

Step5, Calculate the three-dimensional coordinates. // Using the MDS for representative seeds, obtain the three-dimensional coordinates Y.

Step6, Color perception of the representative seeds. // The three-dimensional coordinates Y are rotated by the rotation-scaling matrix R to obtain all seeds with color information, i.e., Y_{rotation} = RY, and R is obtained from the given color information and corresponds to the three dimensional coordinates of some of the seeds.

Step7, Interpolate the seeds to all nodes. // DTI with color information can be obtained by the inter-layer interpolation matrix

P. for k=n:1 $Y_{rotation}^{[k-1]} = P^{[k-1]}Y_{rotation}^{[k]}$

3.5. Analysis of the proposed algorithm

For the DPDR of color perception, the major cost is in the Eigenvalue decomposition and the calculation of the shortest path; thus, the complexity of the DPDR is $O(N^3)$, where N denotes the total number of all pixels. For our proposed method (CPDTI-HML), the selected representative nodes are approximately half of the candidate pixels in every layer. The complexity of interpolation from layer s to s-1 is $O(N^2)$. Thus, the cost of our method is given by the recursive formula: $T(N) = T(\frac{N}{2}) + O(N^2)$, where T(N) represents the time consumed. For T(N), we use the reverse substitution method:

$$T(N) = T\left(\frac{N}{2}\right) + O(N^2) = T\left(\frac{N}{4}\right) + O\left(\frac{N^2}{2}\right) + O(N^2)...$$
$$= T(0) + \sum_{i=0}^{n} O\left(\frac{N^2}{2^i}\right)$$
(14)

Using the limit to approximate the solution:

$$T1(N) = \lim_{n \to +\infty} \sum_{i=0}^{n} O\left(\frac{N^2}{2^i}\right) = O(N^2)$$
 (15)

In [21], from the theorem, the complexity of our proposed method CPDTI-HML is $O(N^2)$.

4. Experimental results

In this section, we will demonstrate the validity of our method by processing the synthetic diffusion tensor images data and the real diffusion tensor images data. Moreover, these experimental results of our proposed method (CPDTI-HML) are compared with three developed methods: Fractional Anisotropy (FA), Mean Diffusivity (MD) [22], and DPDR [9]. In particular, FA and MD are common clinical scalar images. MD represents the average measure of diffusion at a particular direction. MD is the function of the diffusion tensor Eigenvalues λ_i , i=1,2,3, which is defined by the following formula:

$$MD = \overline{\lambda} = \sum_{i=1}^{3} \lambda_i \tag{16}$$

FA represents the proportion of the amount of anisotropy in pixels. FA is defined by:

$$FA = \sqrt{\frac{3}{2}} \sqrt{\sum_{i=1}^{3} (\lambda_i - \bar{\lambda})^2} / \sqrt{\sum_{i=1}^{3} \lambda_i^2}$$
 (17)

To evaluate the performances of the different methods, image entropy is used as the means to measure the uncertainty of the resulting image quantitatively. A larger value of entropy indicates the higher complexity of the images, i.e., its color values are more chaotic. Conversely, a lower value of entropy indicates the image information is

more ordered. The definition of entropy is $Entropy = -\sum_{i=1}^{n} P_i \log P_i$, where P_i denotes the probability of a gray value in the image.

4.1. Results on sunthetic DTI

The synthetic DTI data used for this work are adopted from [9], for which the scan matrix size is 128×128 . For the heat kernel function, we have taken α to be a constant equal to 1. The k-NN is set to 25. To make the representative seeds be approximately half of the candidate nodes in every layer, we set θ to 0.85.

In these synthetic data, the implemented proposed method (CPDTI-HML) was compared with FA, MD, and DPDR [9]. Obviously, scalar images are not able to capture the changes of tensor in direction. Fig. 2 shows the results of using FA, MD, DPDR, and our hierarchy color perception method. From the results, FA is found to only represent the changes along the horizontal direction; however, there is the same value on the same abscissa. For MD, almost no changes are found from the horizontal direction or the vertical direction. Using the DPDR method can capture the changes in the diffusion tensor in both directions by color. The color used in our method can represent the changes of DT in the horizontal direction. However, compared with the FA and MD information presented, our proposed approach can reflect the underlying structure of the original tensor data without introducing error messages, which is of higher clinical value.

4.2. Results on real DTI

The real DTI data corresponds to axial brain DTI slices of a normal subject, and the real DTI data used for this work are from [9], for which the matrix size is 256×256 . For simplicity, all of the parameters of the four compared methods are set to be the same as those in Section 4.1. For slice 1, we have removed the background pixels.

Fig. 3 shows the results of applying the four techniques on the real DTI data, comparing the corresponding FA map, MD map and the result of the DPDR approach with the results of our proposed method. From the experimental results, FA and MD are regarded as gray-scale images, which represent only the simple characteristics and lose a large amount of information. Thus, there are limitations of FA and MD in analyzing the DTI. After processing using the DPDR method and our approach, the white matter and the remaining tissues are separated clearly in the brain image. It is helpful to segment the white matter for subsequent work. However, after the method of DPDR color perception, the result cannot provide a clear distinction with the brain cerebrospinal fluid (CSF) because the approach of DPDR processes all of the pixels and focuses on the difference between pixels rather than the regional structure. Thus, the color is more diverse and the image has rich details, but the regional structure is not obvious. Conversely, our proposed method selects the representative nodes in the similar areas, which pays more attention to color differences between regions. Consequently, the results of our method have obvious regional structure information. From the experimental results of our method with multiple levels, with the layer number increasing, the distinctiveness of the anterior inter-hemispheric and posterior interhemispheric is decreased; and the difference between the white matter and the corpus callosum reduce in the middle part of the images. With the layer number increasing, increasing numbers of pixels are merged into the same areas, which are of similar color. Our results can provide a variety of information for different users..

The other DTI data used in this study consists of three normal subjects; the data are freely available via an online dataset. The data were acquired with following specification: matrix size=128×128, b-value=1000s/mm², number of direction=68.

¹ Available from: http://human.brain-map.org/mri_viewers/data.

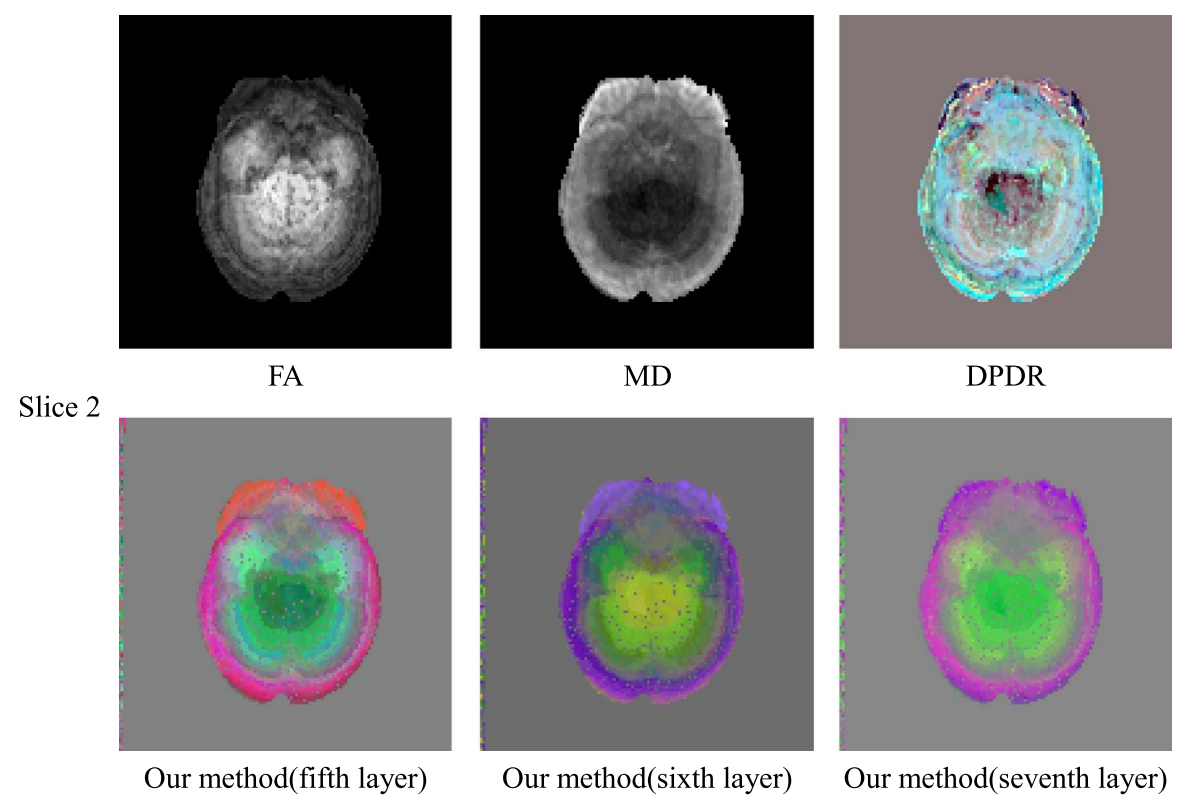


Fig. 4. Qualitative color perception of the DTI slices of a normal subjects. FA, MD, DPDR and our method are displayed. Note that the results of DPDR are chaotic and unclear, whereas our method can reflect the underlying structure, with different regions being marked by different colors. (For interpretation of the references to color in this figure legend, the reader is referred to the web version of this article.)

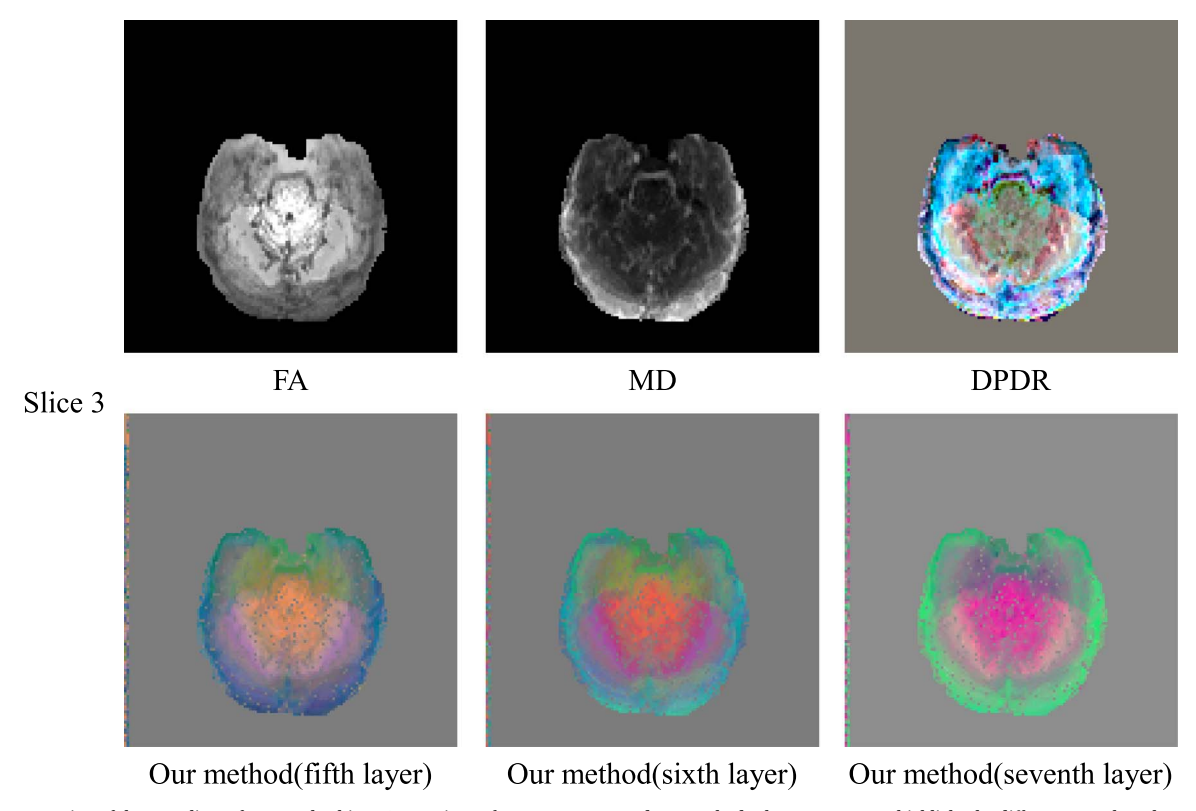


Fig. 5. Color perception of the DTI slices of a normal subject. Comparison of FA, MD, DPDR and our method. The DPDR cannot highlight the different areas by color accurately. Our results express the regional structure clearly, and the multilevel results provide more information. (For interpretation of the references to color in this figure legend, the reader is referred to the web version of this article.)

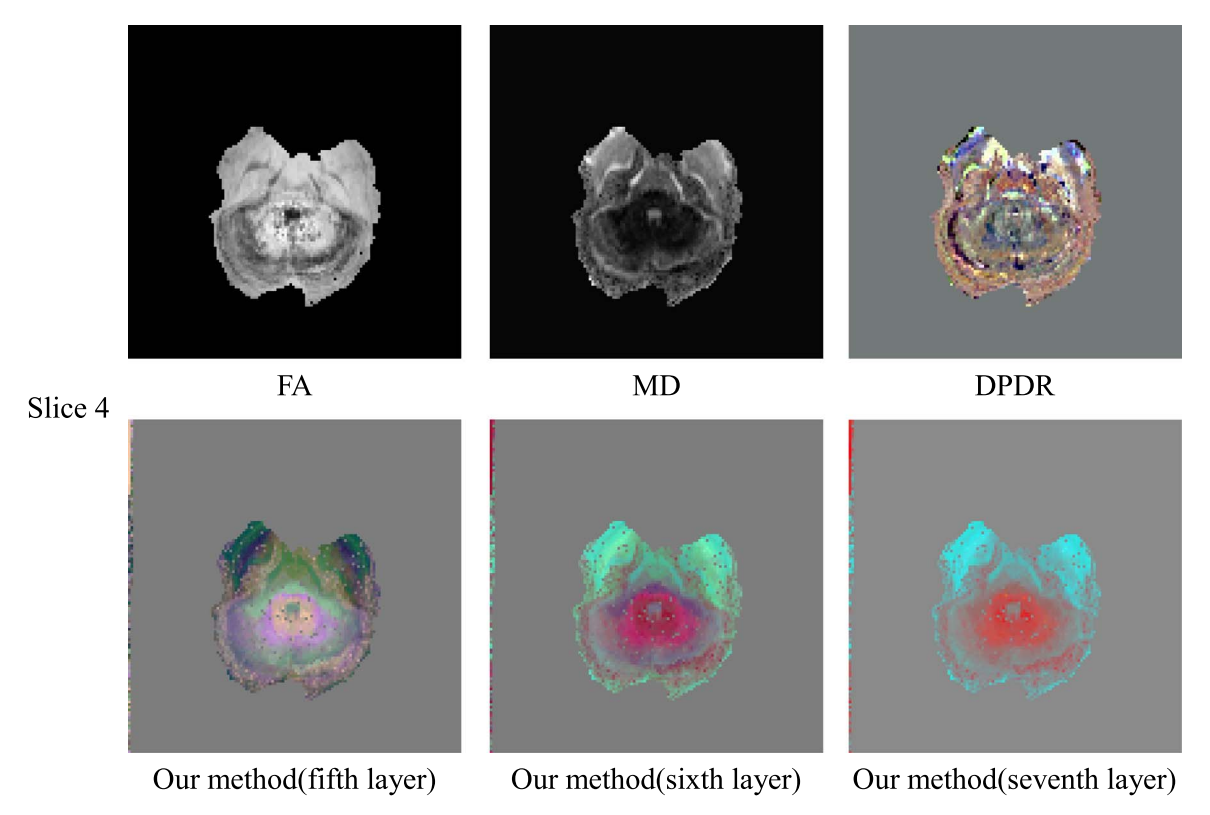


Fig. 6. Qualitative color perception of DTI slices of a normal subject. FA, MD, DPDR and our method are displayed. Our method not only reduces computation but also has noise immunity. The dissimilar color on the perception accurately highlights different areas. (For interpretation of the references to color in this figure legend, the reader is referred to the web version of this article.)

Figs. 4–6 represent the results of FA, MD, DPDR and our approach. We find that FA and MD are gray images and express less information than the color images. Thus, the gray images have lower identification capability than the color images intuitively. When the captured images contain noise, the results of DPDR are chaotic in overall structure, thus failing to render different regions with different color accurately, based on the perception. However, using our method, the results are clear

Table 1The entropy of the four techniques.

Data	Methods									
	FA	MD	DPDR	Fifth Layer	Sixth layer	Seventh layer	Eighth layer			
	Entropy									
Slice 1	3.258	2.915	3.332	_	2.805	3.053	2.917			
Slice 2	3.155	3.081	2.959	2.707	2.742	2.648	_			
Slice 3	2.723	2.673	2.771	2.574	2.055	2.332	_			
Slice 4	2.162	2.186	2.146	2.132	2.073	1.922	_			

regarding the whole image structure, and the different areas are marked accurately by different colors. Thus, using our method makes it possible to efficiently distinguish different parts of tissues and truly reflect the underlying structure and geometrical characteristics....

4.3. Comprehensive analysis of the experiment results

In this section, we will utilize the image entropy to demonstrate the performance of our proposed method (CPDTI-HML) in comparison with another methods and show when building the pyramid, the number of layers is increasing (eventually, the representative seeds are not sufficient), the whole images information aggregation degree.

Table 1 presents a comparison of the information entropy of each approach on real data. It is apparent that the result of our method contains the lower values of the entropy than the results of DPDR, FA and MD. This observation suggests the following: our method provides a regular distribution of color values, the experimental results of CPDTI-HML method has lower uncertainty, and the image structure is clearer as the number of the selected seeds is shown in Table 2.

We utilize the function $information_aggregation_degree$ (i.e. information density degree) to explain the information aggregation

Table 2The distribution of the seeds of each layer in real DTI.

Data	Layers	Layers									
	First layer	Second layer	Third layer	Fourth layer	Fifth layer	Sixth layer	Seventh layer	Eighth layer			
	Seeds										
Slice 1	21367	12305	7184	4184	2427	1411	826	419			
Slice 2	16384	4687	2714	1585	914	533	304	_			
Slice 3	16384	4007	2350	1377	790	456	260	_			
Slice 4	16384	3144	1828	1099	634	376	219	_			

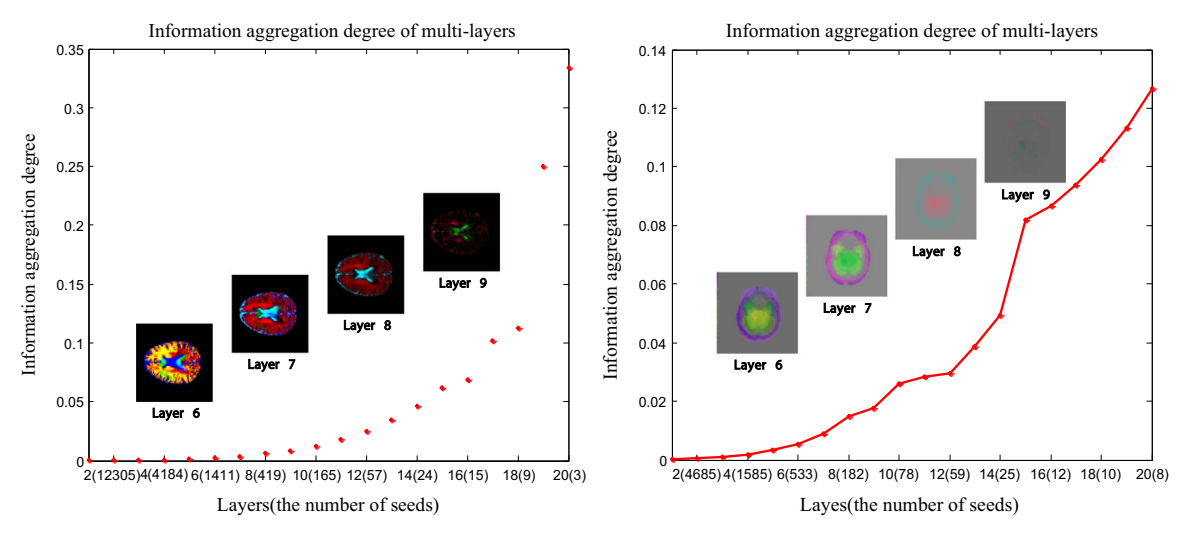


Fig. 7. Display of the information_aggregation_degree of multi-layers (the number in brackets represent the number of seeds corresponding to every layer). With the number of layers increasing, the representative seeds become increasingly few (in the extreme case, only three seeds remain), thereby aggregating a large amount of information of the images, thus rendering the images seriously distorted and meaningless.

for every layer; the function is defined by following formula:

informationaggregationdegree =
$$(\lambda_1 + \lambda_2 + \lambda_3)/N$$
 (18)

where $\lambda_1, \lambda_2, \lambda_3$ are the three largest eigenvalues of the similarity matrix regularization $D^{-1}W$ for every layer, and N represents the total number of representative seeds for every layer. If the $information_aggregation_degree$ is greater value, the more information is aggregated. On the contrary, the lower value of $information_aggregation_degree$ is, the more information is retained.

Now, we analyze the left subfigure in Fig. 7. As shown by the solid line in the Fig. 7, with the number of seeds decreased, more information is aggregated. From layer 1 to layer 8, the change of *information aggregated degree* is smooth; however, after layer 8 (representative seeds are 419), the changes become rapid. In other words, a great deal of information is aggregated from the ninth layer. The subfigure also indicates that the more layers, the more obvious overall regional structures. However, if the number of seeds is too small (only 290 representative seeds or less), the information is excessively aggregated, so that the results only have a few of pixels with color information and the images seriously distorted, and the clinical significance is lost. The results of this paper from the sixth layer to the eighth layer have a lower amount of calculation, while highlighting the structural characteristics. The right subfigure in Fig. 7 is similar regulation.

5. Conclusions

In this paper, we proposed a method for color perception of DTI based on statistical analysis of the voxels combined with the use of the algebraic multigrid to solve the problems of complex computation and the lack of highlighting of the regional structures. The bottom-to-top hierarchical structure is established by selecting the representative seeds. The top-layer seeds are reduced in dimension by MDS using a new distance metric, and then they are converted to the color space directly. Finally, the seeds with color information are interpolated to all pixels to obtain the color perception of all of the pixels.

For both synthetic DTI data and real DTI data, our CPDTI-HML algorithm was compared with FA, MD and DPDR. Our approach not only reduces the complexity but also enhances the areas characteristics, thus improving the identification degrees. In other words, different tissues are marked with different colors on the perception. So far, this technique does not apply to a specific clinical task directly. As a result, the future work will involve cooperation with doctors or radiologists to study and diagnosis diseases of the brain. We hope the proposed algorithm is used in clinical practice in the near future.

Acknowledgments

The author would like to thank the anonymous reviewers for their help. This work was supported by the National Key Research and Development Program of China (Grant no. 2016YFB1000905), the State Key Program of National Natural Science of China (Grant no. U1401252), the National Natural Science Foundation of China (Grant no. 61672120), the Chongqing Natural Science Foundation Program (Grant no. cstc2015jcyjA40036) and Postgraduate Scientific Research and Innovation Project of Chongqing (Grant no. CYS15173).

Appendix A. Supplementary material

Supplementary data associated with this article can be found in the online version at http://dx.doi.org/10.1016/j.patcog.2016.09.021.

References

- P.J. Basser, J. Mattiello, D. Lebihan, MR diffusion tensor spectroscopy and imaging, Biophys. J. 66 (1) (1994) 259–267.
- [2] H. Greenspan, B. van. Ginneken, R.M. Summers, Guest editorial deep learning in medical imaging: overview and future promise of an exciting new technique, IEEE Trans. Med. Imaging 35 (5) (2016) 1153–1159.
- [3] B. G. Booth, Diffusion MRI analysis techniques inspired by the preterm infant brain, D. Applied Sciences: School of Computing Science, 2015
- [4] T. Song, W.J. Chen, B. Yang, H.P. Zhao, J.W. Huang, M.J. Cai, Diffusion tensor imaging in the cervical spinal cord, Eur. Spine J. 20 (3) (2011) 422–428.
- [5] V.Z. Lauren, H.K. Tae, H. Kenneth, M.S. Hill, Using diffusion tensor imaging and immunofluorescent assay to evaluate the pathology of multiple sclerosis, J. Magn. Reson. Imaging 33 (3) (2011) 557–564.
- [6] L. Astola, A. Fuster, L. Florack, A Riemannian scalar measure for diffusion tensor images, Pattern Recognit. 44 (9) (2011) 1885–1891.
- [7] A. Brun, H. J. Park, H. Knutsson and C.-F. Westin, Coloring of DT-MRI fiber traces using Laplacian eigenmaps, in: R. Moreno-Díaz, F. Pichler (Eds.), Processing of Computer Aided Systems Theory (EUROCAST'03), Springer, Verlag, 2003, pp. 518–529
- [8] V. Ragini, K. Parmeshwar, D. Christos, On analyzing diffusion tensor images by identifying manifold structure using isomaps, IEEE Trans. Med. Imaging 26 (26) (2007) 772–778.
- [9] H. Ghassan, M.I. Chris, M.S. Drew, Perception-based visualization of manifold-valued medical images using distance-preserving dimensionality reduction, IEEE Trans. Med. Imaging 30 (7) (2011) 1314–1327.
- [10] B. Yang, M. Xiang, Y. Zhang, Multi-manifold discriminant Isomap for visualization and classification, Pattern Recognit. 55 (2016) 215–230.
- [11] Z.G. Zhu, Y.Y. Kong, Visualization of diffusion tensor images using locality preserving dimensionality reduction, Chin. Med. Equip. J. 34 (6) (2013) 20–22.
- [12] M. H. Aarabi, A. F. Kazerooni, N. Salehi, and S.R. Hamidreza, A high throughput and efficient visualization method for diffusion tensor imaging of human brain white matter employing diffusion-map space, in: Proceedings of the IEEE Engineering in Medicine and Biology Society, 2014, pp. 2368–2371
- [13] A. Abbasloo, V. Wiens, M. Hermann, T. Schultz, Visualizing tensor normal

- distributions at multiple levels of detail, IEEE Trans. Vis. Comput. Graph. 22 (1) (2016) 975–984.
- [14] S.A. Najim, I.S. Lim, Trustworthy dimension reduction for visualization different data sets, Inf. Sci. 278 (10) (2014) 206–220.
- [15] J. Malcolm, Y. Rathi, A. Tannenbaum, A graph cut approach to image segmentation in tensor space, Process. CVPR (2007) 1–8.
- [16] A. Brandt, S. Mccormick, J. Ruge, Algebraic multigrid (AMG) for sparse matrix equations, Sparsity Appl. 13 (3-4) (1984) 257–284.
- [17] M. Galun, E. Sharon, R. Basri, A. Brandt, Texture segmentation by multiscale aggregation of filter responses and shape elements, Process. ICCV (2003) 716–723.
- [18] E. Sharon, A. Brandt, R. Basri, Fast multiscale image segmentation, Process. CVPR 1 (2000) 70–77.
- [19] J.B. Kruskal, Multidimensional scaling by optimizing goodness of fit to a nonmetric hypothesis, Psychometrika 29 (1) (1964) 1–27.
- [20] E. Sharon, M. Galun, D. Sharon, R. Basri, A. Brandt, Hierarchy and adaptivity in segmenting visual scenes, Nature 442 (7104) (2006) 810–813.
- [21] L. Antony, C. Josephine, X. Jane, Introduction to the Design and Analysis of Algorithms, Tsinghua University Press, Bei Jing, 2007, pp. 359–365.
- [22] T. Toshiaki, K. Tesseki, N. Hiroyuki, M. Hirano, Diffusivity and diffusion anisotropy of cerebellar peduncles in cases of spinocerebellar degenerative disease, Neuroimage 37 (2) (2007) 387–393.

Xianhua Zeng is currently a professor with the Chongqing Key Laboratory of Computational Intelligence, College of Computer Science and Technology, Chongqing University of Posts and Telecommunications, Chongqing. He received his Ph.D. degree (supervised by Prof. Siwei Luo) in Computer software and theory from Beijing Jiaotong University in 2009. And he was a Visiting Scholar (supervised by Prof. Dacheng Tao) in the University of Technology, Sydney, from Aug. 2013 to Aug. 2014. His main research interests include machine learning, data mining and medical image processing.

Shanshan He is currently a master degree candidate in the Chongqing Key Laboratory of Computational Intelligence, College of Computer Science and Technology, Chongqing University of Posts and Telecommunications, Chongqing. Her current research interests mainly include manifold learning, medical image analysis.

Weisheng Li is currently a professor with the Chongqing Key Laboratory of Computational Intelligence, College of Computer Science and Technology, Chongqing University of Posts and Telecommunications, Chongqing, China. He received his Ph.D. degree in computer application technology from Xidian University in 2004. His research focuses on intelligent information processing and pattern recognition.



本文献由"学霸图书馆-文献云下载"收集自网络,仅供学习交流使用。

学霸图书馆(www. xuebalib. com)是一个"整合众多图书馆数据库资源, 提供一站式文献检索和下载服务"的24 小时在线不限IP 图书馆。 图书馆致力于便利、促进学习与科研,提供最强文献下载服务。

图书馆导航:

图书馆首页 文献云下载 图书馆入口 外文数据库大全 疑难文献辅助工具